ELSEVIER

Journal of Alloys and Compounds 317–318 (2001) 315–319

Journal of ALLOYS AND COMPOUNDS

www.elsevier.com/locate/jallcom

Crystal growth by molten metal flux method and properties of manganese silicides

Shigeru Okada[a,*], Toetsu Shishido[b], Yoshio Ishizawa[c], Makoto Ogawa[d], Kunio Kudou[e], Tsuguo Fukuda[b], Torsten Lundström[f]

[a]*Faculty of Engineering, Kokushikan University, 4-28-1 Setagaya, Setagaya, Tokyo 154-8515, Japan*
[b]*Institute for Materials Research, Tohoku University, 2-1-1 Katahira, Aoba, Sendai 980-0812, Japan*
[c]*Department of Materials Science, Iwaki Meisei University, 5-5-1 Iino, Chuohdai, Iwaki 970-8551, Japan*
[d]*Faculty of Engineering, Tokyo Institute of Polytechnics, 1583 Iiyama, Atsugi 243-0297, Japan*
[e]*Faculty of Engineering, Kanagawa University, 3-27-1, Rokkakubashi, Kanagawa, Yokohama 221-8686, Japan*
[f]*The Ångström Laboratory, Uppsala University, Box 538, SE-751 21 Uppsala, Sweden*

Abstract

Crystals of binary manganese silicides were grown from high temperature copper, tin and lead metal fluxes by slow cooling method under an argon atmosphere. The growth conditions for obtaining single crystals of relatively large size were established. For tin and lead fluxes, the three silicides Mn_5Si_3, MnSi, and $Mn_{27}Si_{47}$ crystals were prepared, and Mn_5Si_3 (about $0.1\times0.1\times6.4$ mm^3) and MnSi (about $0.9\times1.0\times9.2$ mm^3) were obtained of relatively large size from the tin flux. For copper flux, only the two silicides MnSi and Mn_5Si_3 were formed, and the crystals were somewhat smaller. As-grown Mn_5Si_3, MnSi, and $Mn_{27}Si_{47}$ crystals were used for chemical analyses and measurements of density and unit cell parameters. The chemical analyses of the crystals are discussed. Vickers microhardness and electrical resistivity were determined on MnSi and Mn_5Si_3 crystals, and oxidation at high temperature in air was studied for Mn_5Si_3, MnSi, and $Mn_{27}Si_{47}$ crystals.

Keywords: Mn_5Si_3; MnSi; $Mn_{27}Si_{47}$; Metal flux; Crystal morphology; Electrical resistivity; Vickers microhardness; Thermal properties

1. Introduction

The binary silicides of the transition metals have a high thermal stability, and several unique chemical and physical properties [1]. The disilicides of groups 4–7 transition metals and those of the iron subgroup are of greatest interest. However, the data available on these properties are in most cases obtained from measurements on polycrystalline materials or sintered samples and they are often contradictory. Therefore it is desirable to grow single crystals whose study could give more reliable information on the properties [2]. $MnSi_{2-x}$ crystals have attracted considerable interest because of their remarkable properties and potential for applications as a high temperature thermoelectric material [3]. In the manganese–silicon system the intermediate phases Mn_6Si (rhombohedral), $Mn_{44.10}Si_{8.90}$ (rhombohedral), $Mn_{0.815}Si_{0.185}$ (orthorhombic), Mn_3Si (cubic), Mn_5Si_2 (tetragonal), Mn_5Si_3 (hexagonal), MnSi (cubic), $MnSi_{2-x}$ ($0.250\leq x\leq0.273$: $Mn_{11}Si_{19}$ (tetragonal), $Mn_{26}Si_{45}$ (tetragonal), $Mn_{15}Si_{26}$ (tetragonal), $Mn_{27}Si_{47}$ (tetragonal), and Mn_4Si_7 (tetragonal)) have been reported [3,4]. The Mn–Si phase diagram is that given by Massalski [5]. The simplest method of preparing single crystals of transition metal silicides, in terms of synthesis technology at lower temperature, is provided by the crystal synthesis from solution in metallic melts [2,6–9].

In the present work, we report the growth conditions for Mn_5Si_3, MnSi, and $MnSi_{2-x}$ ($Mn_{27}Si_{47}$) crystals of relatively large size by slowly cooling the copper, tin, and lead metal fluxes. The crystal size, the crystal morphology, densities and crystallographic data of as-grown Mn_5Si_3, MnSi, and $Mn_{27}Si_{47}$ crystals were determined. Electrical resistivity and Vickers microhardness were examined, as well as oxidation resistivity at high temperature in air.

2. Experimental

2.1. Sample preparations

The reagents used to prepare the samples were man-

*Corresponding author.

0925-8388/01/$ – see front matter
PII: S0925-8388(00)01363-3

ganese metal powder (purity, 99.9%), silicon powder (purity, 99.99%), copper chips (99.99%), tin chips (purity, 99.9%), and lead chips (purity, 99.9%). Mn and Si elements were weighed in atomic ratios of range 1:0.5–1:2.0. Metal flux was added to these mixtures at a weight ratio of 15:1. The mixture of these metal elements was placed in an Al_2O_3 crucible and heated under an Ar gas. The temperature of the furnace was raised at a rate of 300°C h^{-1} up to 1200°C and kept for 10 h, and then cooled down at a rate of 50°C h^{-1} to 800°C. Then the furnace was rapidly cooled down to room temperature. The crystals were separated by dissolving the metal fluxes in dilute hydrochloric acid or nitric acid.

2.2. X-ray diffraction and chemical analyses

Relatively large crystals of manganese silicides were selected under a stereomicroscope for crystal size and crystal morphology studies and for chemical analysis. The surfaces of the crystals were analysed in a scanning electron microscope (SEM) (Jeol, JED-2140). The chemical composition of crystals was determined by an electron probe microanalyzer (EPMA) (Jeol, JSM-35C) equipped with an energy dispersive X-ray detector (EDX) (Horiba, EMAX-2770). Possible incorporation of Cu, Sn and Pb atoms into the crystals grown, which might come from the metal solutions, were checked with EDX. The crystalline phases and the unit cell parameters were determined using a powder X-ray diffractometer (XRD) (Rigaku, RINT-2500VHF) with monochromatic CuK_α radiation (wavelength λ=0.154174 nm) and semi-conductor grade silicon (purity, 99.9999%) as internal calibration standard.

2.3. Vickers microhardness and electrical resistivity

As-grown MnSi and Mn_5Si_3 crystals were measured using a Vickers diamond indenter [10] at room temperature. A load of 0.98 N was applied for 15 s at about five points on each crystal, and the values obtained were averaged. The electrical resistivity of as-grown MnSi and Mn_5Si_3 crystals was measured by a direct-current four-probe technique at room temperature in air. The crystals of $Mn_{27}Si_{47}$ were smaller, and not suitable for determination of the microhardness and the electrical resistivity.

2.4. Oxidation resistivity

Thermogravimetric (TG) analysis and differential thermal analysis (DTA) [11] were performed up to 1200°C to study the oxidation resistivity of Mn_5Si_3, MnSi, and $Mn_{27}Si_{47}$ crystals in air. Specimens of about 20 mg were heated at a rate of 10°C min^{-1}. The products obtained by oxidation were analysed by XRD.

Table 1
Preparation conditions of manganese silicide crystals from molten copper flux

Run no.	Starting composition Mn:Si (atomic ratio)	Phases identified
1	1:2.0	MnSi, Mn_5Si_3
2	1:1.74	MnSi, Mn_5Si_3
3	1:1.5	MnSi, Mn_5Si_3
4	1:1.0	MnSi, Mn_5Si_3
5	1:0.5	Mn_5Si_3, MnSi

3. Results and discussion

3.1. Compounds of the Mn–Si system obtained from Cu flux

The atomic ratios Si/Mn in the starting materials were varied from 0.5 to 2.0. The X-ray evidence for the crystalline phases obtained is presented in Table 1. As seen from Table 1, only the two silicides MnSi and Mn_5Si_3 were formed. MnSi crystals were always obtained as a phase mixture together with the Mn_5Si_3 phase. The MnSi and Mn_5Si_3 crystals obtained were small and irregularly-shaped polyhedral crystals.

3.2. Compounds of the Mn–Si system obtained from Sn flux

The X-ray evidence for the crystalline phases obtained is listed in Table 2. As seen from Table 2, Mn_5Si_3, MnSi, $Mn_{27}Si_{47}$ and Si phases were formed. The variation of the atomic ratio of the starting materials gave different product phases. With increased silicon concentration, more silicon-rich phases are obtained. Three manganese silicides Mn_5Si_3, MnSi and $Mn_{27}Si_{47}$ were obtained as single crystals. The crystals of all three phases had a grayish color and metallic lustre. Prismatic crystals of Mn_5Si_3 were generally obtained extending in the ⟨0001⟩ direction (Fig. 1A). MnSi single crystals were generally obtained as prisms extending in ⟨100⟩ direction (Fig. 1B), while $Mn_{27}Si_{47}$ single crystals had a nearly spherical polyhedral shape (Fig. 1C). The largest Mn_5Si_3 crystals had maximum dimensions of about 0.1×0.1×6.4 mm^3. The largest MnSi and $Mn_{27}Si_{47}$ crystals had maximum dimensions of about 0.9×1.0×9.2 mm^3 and 0.25×0.25×0.25 mm^3, respectively. The electrical resistivity, Vickers microhard-

Table 2
Preparation conditions of manganese silicide crystals from molten tin flux

Run no.	Starting composition Mn:Si (atomic ratio)	Phases identified
6	1:2.0	$Mn_{27}Si_{47}$, Si
7	1:1.74	$Mn_{27}Si_{47}$, Si
8	1:1.5	$Mn_{27}Si_{47}$, MnSi
9	1:1.0	MnSi
10	1:0.5	Mn_5Si_3, MnSi

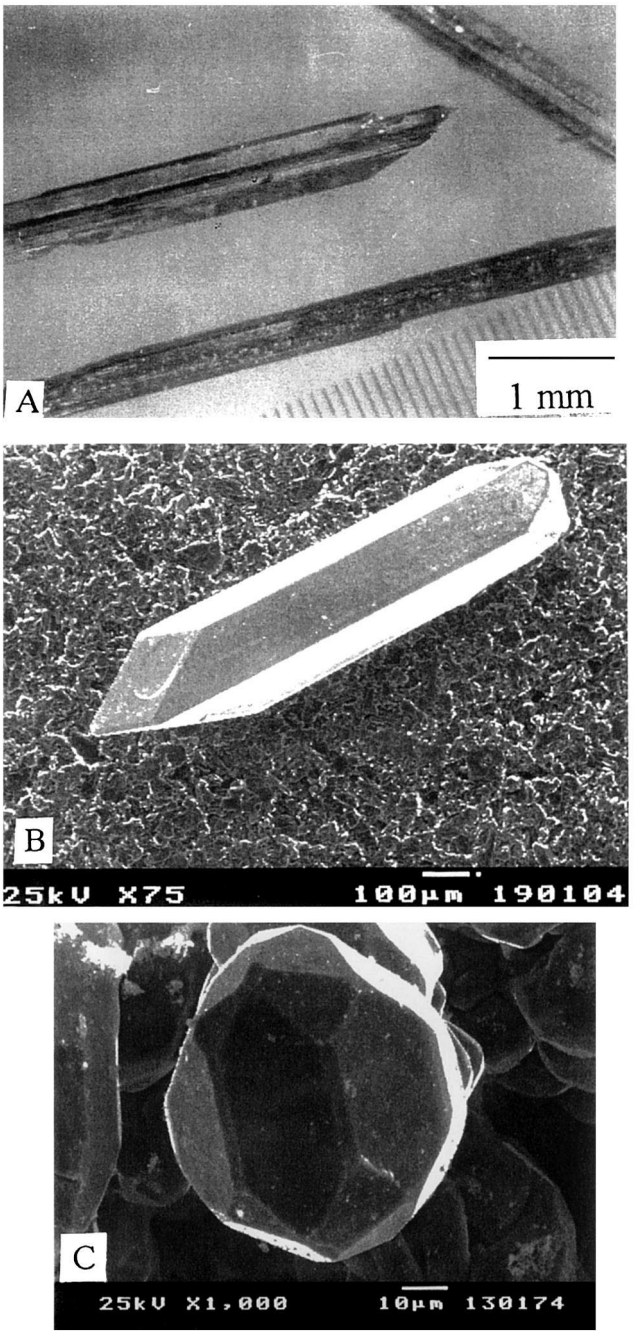

Fig. 1. Microphotograph and SEM photographs of Mn_5Si_3 (A) (run no. 10), MnSi (B) (run no. 9), and $Mn_{27}Si_{47}$ (C) (run no. 7) crystals grown by the tin flux method.

ness and TG-DTA measurements were performed on the largest crystals.

3.3. Compounds of the Mn–Si system obtained from Pb flux

The X-ray evidence for the crystalline phases obtained is presented in Table 3. As seen from Table 3, four compounds Mn_5Si_3, MnSi, $Mn_{27}Si_{47}$ and Si phases were

Table 3
Preparation conditions of manganese silicide crystals from molten lead flux

Run no.	Starting composition Mn:Si (atomic ratio)	Phases identified
11	1:2.0	Si, $Mn_{27}Si_{47}$
12	1:1.74	$Mn_{27}Si_{47}$, MnSi
13	1:1.5	$Mn_{27}Si_{47}$, MnSi
14	1:1.0	MnSi, Mn_5Si_3
15	1:0.5	Mn_5Si_3, MnSi

formed. It is shown that the more silicon-rich phases form for the larger Si/Mn values in the starting materials in a similar manner to that observed in Sn flux. $Mn_{27}Si_{47}$ crystals were obtained as a phase mixture together with MnSi or Si crystals, and MnSi crystals were always obtained as a phase mixture together with Mn_5Si_3 crystals. Mn_5Si_3 and MnSi crystals were smaller, and generally obtained as irregularly shaped crystals. $Mn_{27}Si_{47}$ were obtained as nearly spherical polyhedral single crystals (Fig. 2) and the largest crystals had maximum dimensions of about 50 µm.

3.4. Unit cell parameters, densities and compositions of manganese silicides

The basic crystal data, densities and chemical compositions of manganese silicides are listed in Tables 4 and 5. The unit cell parameters of Mn_5Si_3, MnSi and $Mn_{27}Si_{47}$ crystals obtained are in good agreement with previously published data [3]: for Mn_5Si_3 $a=0.6910$ nm, $c=0.4814$ nm; for MnSi $a=0.4557$ nm; for $Mn_{27}Si_{47}$ $a=0.5530$ nm, $c=11.794$ nm. The EPMA or EDX results seem to indicate that the manganese silicides have appreciable homogeneity ranges. The expected variations of the unit cell parameters with composition were not observed, however, and thus conclusive evidence for homogeneity ranges is not re-

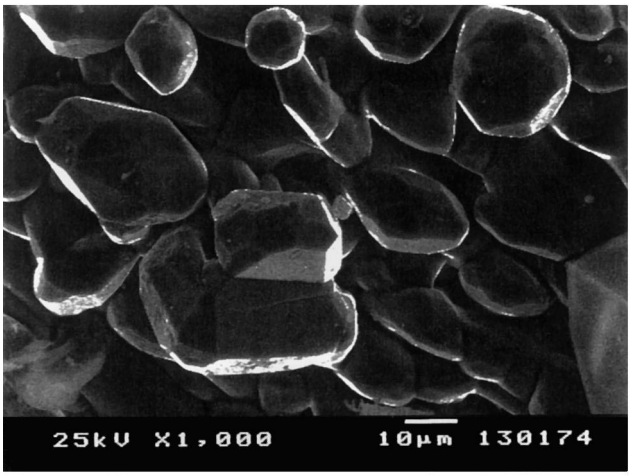

Fig. 2. SEM photograph of $Mn_{27}Si_{47}$ (run no. 12) crystals grown by the lead flux method.

Table 4
The unit cell parameters and densities of manganese silicide crystals

Metal flux	Cu	Cu	Sn	Sn	Sn	Pb	Pb	Pb
Run no.	1	5	7	9	10	12	14	15
Formula unit	MnSi	Mn_5Si_3	$Mn_{27}Si_{47}$	MnSi	Mn_5Si_3	$Mn_{27}Si_{47}$	MnSi	Mn_5Si_3
Crystal system	Cubic	Hexagonal	Tetragonal	Cubic	Hexagonal	Tetragonal	Cubic	Hexagonal
a (nm)	0.4559(1)	0.6911(2)	0.5530(1)	0.4558(1)	0.6909(2)	0.5529(1)	0.4559(1)	0.6910(1)
b (nm)	–	–	–	–	–	–	–	–
c (nm)	–	0.4814(1)	11.786(2)	–	0.4815(1)	11.784(2)	–	0.4815(1)
V ($\times 10^{-3}$ nm^3)	94.76(1)	199.12(1)	3604.26(2)	94.69(1)	199.04(2)	3602.35(2)	94.76(1)	199.10(1)
Space group	$P2_13$	$P6_3/mcm$	$P\bar{4}n2$	$P2_13$	$P6_3/mcm$	$P\bar{4}n2$	$P2_13$	$P6_3/mcm$
Z	4	2	4	4	2	4	4	2
d_m (g cm^{-3})[a]	–	–	5.17(2)	5.80(1)	5.95(2)	–	–	–
d_x (g cm^{-3})	5.819(1)	5.987(1)	5.166(1)	5.818(1)	5.989(1)	5.169(1)	5.820(1)	5.988(1)

[a] Pycnometer method with distilled water at 20°C.

Table 5
The results of the chemical analysis of manganese silicide crystals

Metal flux	Cu	Cu	Sn	Sn	Sn	Pb	Pb	Pb
Run no.	1	5	7	9	10	12	14	15
Formula unit	MnSi	Mn_5Si_3	$Mn_{27}Si_{47}$	MnSi	Mn_5Si_3	$Mn_{27}Si_{47}$	MnSi	Mn_5Si_3
Mn (wt.%)[a]	–	–	53.8	65.8	78.1	53.5	–	–
Si (wt.%)[a]	–	–	46.2	34.2	21.9	46.5	–	–
Chemical composition	–	–	$Mn_{27.98}Si_{47}$	$Mn_{0.98}Si$	$Mn_{5.45}Si_3$	$Mn_{27.64}Si_{47}$	–	–

[a] EPMA or EDX results.

ported. Although the impurity content of Mn_5Si_3, MnSi and $Mn_{27}Si_{47}$ crystals was not analysed chemically, the EPMA and EDX established the occurrence of traces of calcium, magnesium, iron and aluminium, while copper, tin and lead as metal flux were found to lie below the detection limit (<0.05%). Consequently, the solid solubility of copper, tin or lead in manganese silicides is extremely low.

3.5. Hardness and electrical resistivity

The Vickers microhardness of as-grown Mn_5Si_3 and MnSi crystals was measured on the (10$\bar{1}$0) and (100) planes, respectively. As listed in Table 6, the value of the Vickers microhardness for manganese silicides are distributed over 8–11 GPa. The microhardness values of Mn_5Si_3 are somewhat lower than the value of MnSi. The microhardness value of Mn_5Si_3 and MnSi crystals were not reported in the literature earlier.

The electrical resistivity of as-grown Mn_5Si_3 and MnSi crystals was measured parallel to ⟨0001⟩ and ⟨100⟩ direction. The electrical resistivities are listed in Table 7 together with previously published data [3]. Mn_5Si_3 and MnSi crystals show nearly the same electrical resistivity.

Table 7
Electrical resistivity of Mn_5Si_3 and MnSi crystals

Sample	Run no.	Electrical resistivity ($\mu\Omega$ cm)	Refs.
Mn_5Si_3	10	3500±230	This work
Mn_5Si_3	–	257±14	[3]
MnSi	9	3200±180	This work
MnSi	–	259±12	[3]

The values of Mn_5Si_3 and MnSi crystals are an order of magnitude higher than those earlier reported. The literature values of manganese silicides appear to have been obtained from a polycrystalline compound.

3.6. TG-DTA measurement

Mn_5Si_3, MnSi and $Mn_{27}Si_{47}$ crystals of sizes in the range 105–180 μm were used to examine the oxidation of crystals in air. The process of oxidation of the crystals was studied at temperatures below 1200°C by TG-DTA, as shown in Fig. 3. The oxidation reaction of the Mn_5Si_3, MnSi and $Mn_{27}Si_{47}$ crystals from TG curves starts at about 860°C, 1060°C and 760°C, respectively. The weight gain of MnSi is small (3.5%) and therefore it was not possible

Table 6
Vickers microhardness of Mn_5Si_3 and MnSi crystals

Sample	Run no.	Crystal structure	Indentation plane	Vickers microhardness (GPa)
Mn_5Si_3	10	Hexagonal	(10$\bar{1}$0)	7.8–8.3
MnSi	9	Cubic	(100)	10.4–11.2

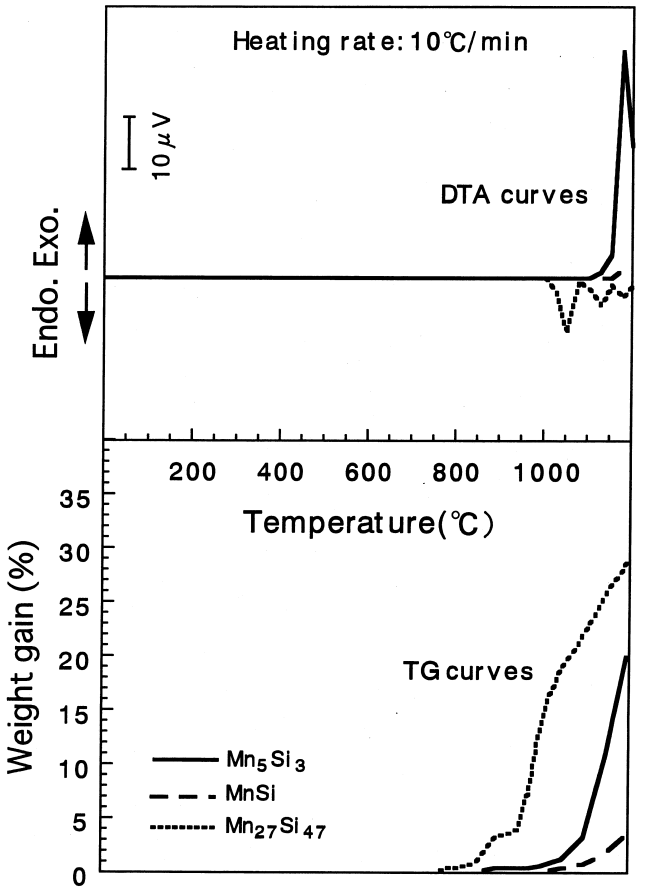

Fig. 3. TG-DTA curves of Mn_5Si_3, MnSi, and $Mn_{27}Si_{47}$ crystals heated in air.

to identify any oxidation products by XRD. MnSi (cubic system) shows high oxidation resistivity, while $Mn_{27}Si_{47}$ (tetragonal system) and Mn_5Si_3 (hexagonal system) show low oxidation resistivity. The resistivity towards oxidation seems to be related to crystal structure and thermodynamic stability. However, a large exothermic peak of the DTA curve was found at about 1175℃ for Mn_5Si_3, and three small endothermic peaks of the DTA curve were found at about 1023℃, 1125℃ and 1176℃ for $Mn_{27}Si_{47}$. The following oxidation products were identified for Mn_5Si_3 as well as $Mn_{27}Si_{47}$, namely crystalline $MnSiO_3$ (triclinic), MnO (cubic), γ-Mn_2O_3 (tetragonal) and SiO_2 (tetragonal). For Mn_5Si_3 this leads to the following total formula:

$$Mn_5Si_3 + 6O_2 \rightarrow MnSiO_3 + 2MnO + \gamma\text{-}Mn_2O_3 + 2SiO_2$$

The observed weight gain of about 30% at 1200℃ (Fig. 3) corresponds to a transformation of ~50% by volume of the Mn_5Si_3 crystals. This reaction is probably exothermic. The occurrence of three small endothermic peaks in the DTA curve of $Mn_{27}Si_{47}$ is probably associated with partial melting of the $MnSi_{2-x}$ phase. However, the phase relationships ($Mn_{11}Si_{19}$, $Mn_{15}Si_{26}$, $Mn_{26}Si_{45}$, and $Mn_{27}Si_{47}$) and the corresponding part of the phase diagram [12] are not well known and conclusions are uncertain.

4. Conclusion

In this investigation crystals of manganese silicides Mn_5Si_3, MnSi, and $Mn_{27}Si_{47}$ were prepared from a high temperature flux method using copper, tin or lead as fluxes. From copper flux, only the two silicides MnSi and Mn_5Si_3 were formed. Crystals of other phases were smaller, and not sufficiently large for property measurements. From tin and lead fluxes, the three silicides Mn_5Si_3, MnSi, and $Mn_{27}Si_{47}$ crystals were prepared. The largest crystals were those of Mn_5Si_3 and MnSi as obtained from tin flux. These crystals were of mm size. The oxidation sets in at relatively high temperature for MnSi, namely at 1060℃. As-grown manganese silicide crystals were used for measurements of Vickers microhardness and electrical resistivity. In this study, the electrical resistance of Mn_5Si_3 and MnSi crystals were found to be an order of magnitude higher than earlier reported, based on sintered bodies [3]. The microhardness values of Mn_5Si_3 are somewhat lower than the value of MnSi. The microhardness values of the compounds seem to be related to its crystal structure.

Acknowledgements

The authors would like to thank Dr. K. Iizumi, Miss T. Tsuchiya and Mr. F. Matsukawa of Tokyo Institute of Polytechnics, and Dr. L.-E. Tergenius of Uppsala University for their help in the experiments.

References

[1] B. Aronsson, T. Lundström, S. Rundqvist, in: Borides, Silicides and Phosphides, Methuen, London, 1965, p. 1.
[2] P. Peshev, M. Khristov, G. Gyurov, J. Less-Common Metals 153 (1989) 15.
[3] G.V. Samsonov, I.M. Vinitskii, in: Handbook of Refractory Compounds, IFI/Plenum, New York, 1980, p. 136.
[4] P.F. Wieser, W.D. Forgeng, Trans. AIME 230 (1964) 1675.
[5] T.B. Massalski, in: 2nd Edition, Binary Alloy Diagrams, Vol. l, The Material Information Society, ASM International, Ohio, 1990, p. 1588.
[6] S. Okada, T. Atoda, Nippon Kagaku Kaishi 5 (1983) 746, in Japanese.
[7] S. Okada, K. Kudou, M. Miyamoto, Y. Hikichi, Nippon Kagaku Kaishi 12 (1991) 1612, in Japanese.
[8] S. Okada, K. Kudou, T. Lundström, in: Proceedings of the Sixth International Conference on Ferrite (ICF 6), 1992, p. 389.
[9] S. Okada, K. Okita, K. Hamano, T. Lundström, High Temp. Mater. Processes 13 (1994) 311.
[10] S. Okada, T. Atoda, I. Higashi, Y. Takahashi, J. Less-Common Metals 113 (1985) 331.
[11] S. Okada, K. Iizumi, K. Kudaka, T. Shishido, T. Fukuda, in: 9th Cimtec-World Forum on New Materials Symposium VII — Innovative Materials in Advanced Energy Technologies, Vol. 24, 1999, p. 635.
[12] T.B. Massalski (Ed.), Binary Phase Diagrams, American Society of Metals, Metals Park, OH, USA, 1986, p. 1588.